Covalency in oxidized uranium

J. G. Tobin* and S.-W. Yu
Lawrence Livermore National Laboratory, Livermore, California 94550, USA

R. Qiao, W. L. Yang, C. H. Booth, and D. K. Shuh
Lawrence Berkeley National Laboratory, Berkeley, California 94720, USA

A. M. Duffin
Pacific Northwest National Laboratory, Richland, Washington 99354, USA

D. Sokaras, D. Nordlund, and T.-C. Weng
Stanford Synchrotron Radiation Lightsource, Stanford, Menlo Park, California 94025, USA
(Received 15 April 2015; published 29 July 2015)

Using x-ray emission spectroscopy and absorption spectroscopy, it has been possible to directly access the states in the unoccupied conduction bands that are involved with $5f$ and $6d$ covalency in oxidized uranium. By varying the oxidizing agent, the degree of $5f$ covalency can be manipulated and monitored, clearly and irrevocably establishing the importance of $5f$ covalency in the electronic structure of the key nuclear fuel, uranium dioxide.

DOI: 10.1103/PhysRevB.92.045130 PACS number(s): 78.70.En, 71.20.Gj, 71.20.Ps, 78.70.Dm

I. INTRODUCTION

Actinides, the $5f$ elements and their compounds, alloys, and mixtures, are a crucially important part of modern technological societies [1–3]. Moreover, uranium dioxide is the most widely used nuclear fuel for the generation of electricity [1]. Yet, because of the complexity of the $5f/6d$ electronic structure in the actinides, a fundamental understanding of their physical behavior, in actinides in general and uranium dioxide in particular, has not been achieved. This could potentially limit the utility of simulations of UO_2 that are part of the safety framework for disposal and storage, and energy production. It is of paramount importance that the models for UO_2 be properly benchmarked with experimental results, both because of the issue of fundamental scientific understanding and because of the absolute requirement of the accuracy of computational simulations for safety issues.

Theoretically, it has been proposed that covalency is an important part of the electronic structure of actinide dioxides [4], although some disagree [5]. Experimentally, spectroscopic studies have been reported which support the hypothesis of $5f$ covalency [6,7]. However, a crucially important and absolutely essential component has been missing: a systematic study where the nature of the oxidant is changed, so the specifics of the $5f$ and $6d$ covalencies could be varied and monitored. The turning-on and turning-off of an effect is the essence of a true benchmarking. The work reported here clearly and irrevocably establishes experimentally the strong presence of U $5f$–O $2p$ covalency in the unoccupied density of states of UO_2, the most important of our nuclear fuels.

Fluorine is a very reactive and dangerous element [8]. Its halogen cousins, chlorine and iodine, have common usage as oxidizing agents among the general population, e.g., in swimming pools and clean wipes for chlorine, and water purification and wound disinfectant for iodine. However, fluorine's propensity to oxidize is so strong that it ends up being used in applications such as rocket fuel. Moreover, it has a very dangerous side and can be a threat to human well-being. For example, exposure to hydrofluoric acid causes systemic poisoning that can result in death, with local applications sometimes leading to amputations.

Thus this comparative study will feature the isoelectronic systems uranium dioxide (UO_2) and uranium tetrafluoride (UF_4). While isoelectronic, both being U^{+4} $5f^2$ in the formal limit [9], they exhibit substantially different structures. UO_2 is a fluorite (cubic) material, while UF_4 is monoclinic [10]. However, both exhibit very similar U L_3 extended x-ray absorption fine structure (EXAFS) behavior, indicative of quantitatively similar interatomic distances [10]. UF_4 has been studied before with x-ray absorption [11], but these new measurements are complementary to the earlier study [e.g., FK($1s$) x-ray absorption spectroscopy (XAS)], and have been performed with improved resolution and over a more extensive energy range [e.g., the U L_3 ($2p_{3/2}$) x-ray absorption fine structure, both x-ray absorption near edge structure (XANES) and EXAFS] [10,12]. The result of this comparative study is that UF_4 exhibits continued $6d$ covalency but the almost complete loss of $5f$ covalency, while UO_2 clearly displays both strong $5f$ and $6d$ covalencies. Here we have direct experimental demonstration that $5f$ covalency is important in actinide oxides but can be lost with a more powerful oxidizing agent such as fluorine.

II. EXPERIMENT

The x-ray measurements were performed upon three beamlines: BL 8.0 at the Advanced Light Source (ALS) at Lawrence Berkeley National Laboratory (LBNL); BL 6-2 and BL 11-2, both at the Stanford Synchrotron Radiation Lightsource (SSRL). For BL 8.0, energy calibrations were performed at the Fe $2p_{3/2}$ white line (710 eV for iron oxide)

*Corresponding author: Tobin1@LLNL.Gov

for the beamline monochromator and at the FK($1s$) at 675 eV [1] for the fluorescence monochromator and detector. Details of the BL 8.0 characteristics can be found in Ref. [13]. The partial fluorescence yield (PFY) U L_3 data [14,15] were collected at SSRL wiggler beamline 6-2 using an LN_2-cooled Si(311) double monochromator calibrated so that the inflection point of the Zr K-edge absorption from a Zr reference foil was at 17 998.0 eV. The emission energy was measured using a seven-crystal Ge(777) Johann-type x-ray emission [16] spectrometer at an emission energy of approximately 13.6 keV, corresponding to the U $L_{\alpha 1}$ fluorescence. The energy of the emission spectrometer was calibrated with elastic scattering peaks, while the incident beam (beamline) monochromator was calibrated at the Au L_2-edge absorption edge (13 734.0 eV) using a Au reference foil. Data were collected at room temperature (300 K). The experimental resolution was 1.7 eV at the U $L_{\alpha 1}$ emission energy, which is dominated by the broadening due to the $3d_{5/2}$ core hole of about 3.5 eV [12]. The conventional XANES U L_3-edge data [10] were collected in fluorescence mode from the U L_α line on BL 11-2 at SSRL, with a half-tuned double Si(220) ($\varphi = 0°$) LN_2-cooled monochromator on unfocused beam and a 100-element Ge solid-state detector [17], with the sample at $T = 50$ K. The effective linewidth in the conventional XANES measurements is dominated by the $2p_{3/2}$ core-hole lifetime broadening of about 8 eV [10,12], much greater than the PFY XANES. The uranium dioxide sample used in Ref. [7] was polycrystalline with a well-defined surface [1,6,7]. The uranium tetrafluoride was a single-crystalline sample, with significant surface degradation [1]. The surface degradation will be shown to be irrelevant.

III. RESULTS AND DISCUSSION

In two earlier studies, strong evidence of $5f$ and $6d$ covalency was found in UO_2. First, XAS was used to show that the unoccupied states of uranium and oxygen overlapped in a significant way, suggesting that there was both U $5f$–O $2p$ hybridization and U $6d$–O $2p$ hybridization [6]. Second, a detailed study with resonant inverse photoelectron spectroscopy (RIPES) was performed, which provided another confirmation of the splitting of the uranium unoccupied density of states (UDOS) into two subbands for the U $5f$ and U $6d$ states. Moreover, it was found that the U $4d$ x-ray emission spectroscopy (XES) provided essentially the same information, without the limitation of the strong surface sensitivity of RIPES. While the electron gymnastics are clear and simple for RIPES, the mechanisms to explain the effect for XES must rely upon the availability and flow of background electrons. For example, one possible mechanism for this XES process is discussed in Ref. [1]. An alternative but very closely related picture would be the following. While the decay process of XES provides a measure of the occupied density of states (ODOS), *it is the ODOS in the presence of a core hole*. It is a known that increasing the nuclear charge in the actinides can shift binding energies of near-valence core states such as the $5d$'s, $5p$'s, and $4f$'s by $\sim$10 eV/unit charge or more [18]. Thus, in the process of ionization, the original low-lying UDOS could now be occupied and the $4d$ XES could provide a measure of the original low-lying UDOS. These results are summarized in Fig. 1.

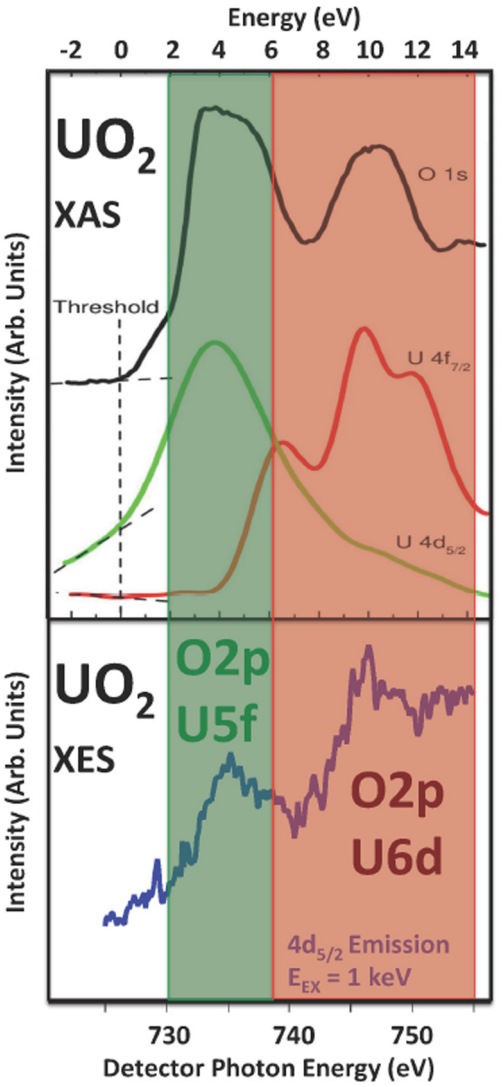

FIG. 1. (Color online) The unoccupied density of states (UDOS) of UO_2, as determined from the O $1s$, U $4f$, and U $4d$ XAS and the U $4d$ XES is shown here. See text for details. Here, the XES is performed in house using an electron gun for excitation [7].

To extend the measurements to UF_4, an operational change was necessary. While the UO_2 sample used in Ref. [7] had a well-defined and clean surface, the UF_4 sample would not be thus. It is possible to sputter clean the surface of a UF_4 sample, but then the stoichiometry would be ruined. Rather than change the stoichiometry, it was decided to probe the UF_4 only with spectroscopies that could sample bulk behavior. For example, as reported earlier, while x-ray photoelectron spectroscopy (XPS) could only see uranium, oxygen, and carbon on the surface of the UF_4 sample, the F $1s$ XES was clearly and strongly visible [1]. Interestingly, it is important that there is little or no F on the surface; this means that the F signal will be coming from the bulk. This issue will be revisited later.

Consider the spectra in Fig. 2. In the top panel, there is the XES for the detector photon energy region of 660–760 eV, using an excitation photon energy of 810 eV. The detector energy

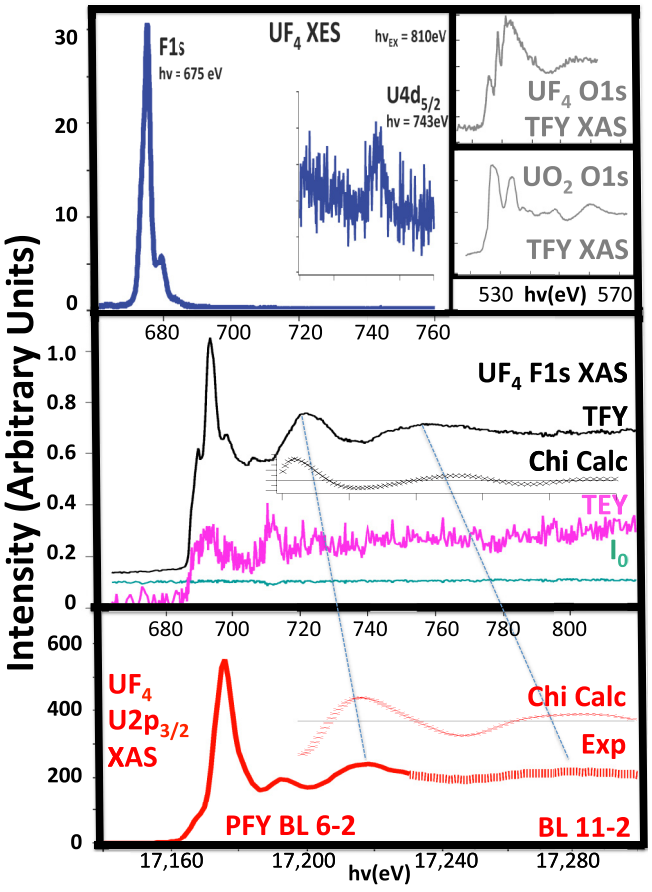

FIG. 2. (Color online) The XES and XAS of UF_4, plus supporting measurements and calculations, are displayed here. See text for details. The solid part of the U $2p$ data is from beamline 6-2 [12] and the dashed from beamline 11-2 [10]. TFY is total fluorescent yield. TEY is total electron yield. I_0 is a measure of the beamline photon intensity. The χ_{Calc} curves for the F $1s$ and U $2p_{3/2}$ are deviations from zero, shown as a horizontal line in each case. Each of the χ_{Calc} curves were generated using FEFF based upon a cluster model for UF_4 and each curve here runs from KE (kinetic energy) $=20$ eV to KE $= 120$ eV. The U $2p_{3/2}\chi_{\mathrm{Calc}}$ (F $1s\,\chi_{\mathrm{Calc}}$) curve in this range has a minimum value of -0.15 (-0.07) and a maximum value of 0.10 (0.21). The U $2p_{3/2}\chi_{\mathrm{Calc}}$ (F $1s\,\chi_{\mathrm{Calc}}$) curve has a calculated value of $E_F = 17\,164.58$ eV (680.84), but the plot uses E_F near 17 150 eV (695 eV) for the comparison to the experiment. The slanted, dashed blue lines show the positions of the EXAFS oscillations, as indicated by the χ function obtained from an FEFF calculation [22].

here is calibrated upon similar measurements made in house of the FK($1s$) XES [1]. The F $1s$ peak is strong and well defined, very similar to the F $1s$ peak in Ref. [1]. The U $4d$ peak, shown in the blowup, is at least 3 orders of magnitude weaker but still visible above the noise. Clearly, there is only one major peak here, already different than the result for uranium dioxide. Because the XPS showed no surface peak, it is safe to conclude that the F $1s$ XES is solely derived from the bulk. It is important that the F $1s$ and U $4d$ features were collected in one scan, eliminating the issue of energy calibration for an isolated U $4d$ peak. While time consuming (8–12 h), it permits the overlay of peaks that will be utilized below. Similarly, a wide XAS spectrum was collected for the uranium tetrafluoride, shown in the middle panel. Here the energy calibration is based upon the Fe $2p$ of iron oxide, which can be seen in both the I_0 and total electron yield (TEY) curves. TEY is fairly surface sensitive. The poor quality of the TEY is a reminder and confirmation of the corrosion of the outside of the uranium tetrafluoride sample. This can be further confirmed by looking at the O $1s$ XAS of the UF_4 sample, shown in an insert in the upper-right corner. Oxygen should not be present in the uranium tetrafluoride, so the observation of any O $1s$ intensity is indicative of surface corruption. Moreover, the three-peak spectral structure is reminiscent of the O $1s$ spectra of UO_3 of Magnuson *et al.* [19], the $(AnO_2Cl_4)^{-2}$ uranyl compounds reported by Clark [20], and the UO_2F_2 of the Pacific Northwest National Laboratory (PNNL) group [21], not at all like our O $1s$ from uranium dioxide, also shown in the corner inset. Thus some of the corrosion may be in the form of UO_2F_2 or UO_3 or an analogous uranyl structure. In contrast to the surface-sensitive TEY, the total fluorescence yield exhibits a plethora of fine structure, which is all easily understandable. As with the XES, the total fluorescence yield (TFY) measurements are all photon based and thus bulk sensitive. One can clearly see the detailed spectral features near the F $1s$ threshold near 690 eV. In addition to the sharp peaks due to the electronic transitions described below, there are also EXAFS features that dominate the spectrum about 20 eV beyond the main peak. Both the FK($1s$) and the $UL_3(2p_{3/2})$ EXAFS are consistent with that expected for the nominal UF_4 structure, as shown by the FEFF 10.0 [22] calculation of the EXAFS function χ [23], shown in Fig. 2. It is also worth noting that the F $1s$ EXAFS from UF_4 and the O $1s$ EXAFS from UO_2 are very similar, paralleling the strong similarities in their L_3 EXAFS [10]. There should be U $4d_{5/2}$ XAS (about 736 eV) and U$4d_{3/2}$ XAS (about 778 eV) peaks [11,12]. However, as suggested by the XES results, these peaks will be small relative to the F $1s$ XAS. Moreover, all of the uraniums will contribute, thus broadening the already-weak features with shifts from the chemical inhomogeneity of the different forms of uranium. Hence, the likelihood of seeing a U $4d$ XAS peak is small, and instead, these will manifest themselves as broadening in the F $1s$ EXAFS. It should also be noted that the strong F $1s$ EXAFS is supportive of the contention that the F $1s$ intensity is bulk derived, being so clearly associated with the L_3 EXAFS from bulk uranium fluoride. (Finally, similar F $1s$ XAS and O $1s$ XAS data were collected at the University of Wisconsin Synchrotron Radiation Center using a different UF_4 sample with lessened surface damage [24].) Next, the data from these measurements are overlaid in a fashion similar to the data in Fig. 1.

Consider now the overlay of spectra in Fig. 3 for the uranium tetrafluoride sample. To align the XAS spectra, we used the threshold method, developed earlier for uranium dioxide [6]. Here, instead of using the low-energy $4f$ XAS to access the $6d$ UDOS, the bulk sensitive L_3 $(2p_{3/2})$ XAS has been utilized. Again, this method is dependent upon the dominance of electric dipole selection rules, as in Ref. [6]. The energy scale on the lower panel is determined by that used in the analysis of the uranium dioxide [1,7] and the alignment of the F $1s$ peaks in the in-house and ALS experiments and the utilization of the inclusive wide scan in Fig. 2. The U $4d$

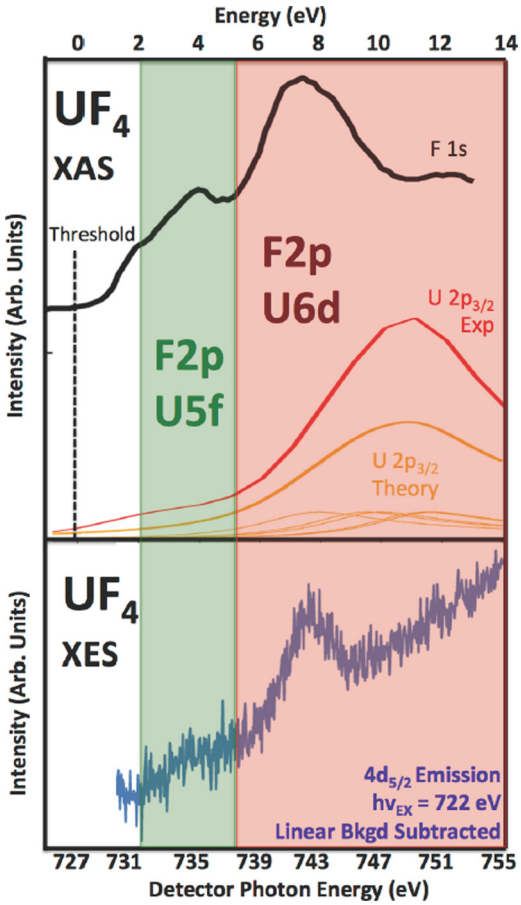

FIG. 3. (Color online) The unoccupied density of states (UDOS) of UF_4 as determined from the F 1*s* and U 2*p* XAS and the U 4*d* XES is shown here. A simulated U 2*p* spectrum is also included, with the underlying states from the Ryzhkov cluster calculations [25,26]. See text for details.

XES spectra were measured at several excitation energies, always producing the result of a single, fairly strong peak at $h\nu_{\mathrm{DET}} = 743$ eV, often with the suggestion of a weaker feature at slightly lower photon energy. Shown in Fig. 3 are data that were collected at $h\nu_{\mathrm{EX}} = 722$ eV, with an extended data collection period to reduce the noise. This energy is seemingly below threshold, but as reported earlier [1], the wide lifetime broadening in these XES events permits excitations with lower energies. At $h\nu_{\mathrm{EX}} = 722$ eV, there is clearly a second but very weak feature at about $h\nu_{\mathrm{DET}} = 735$ eV. This feature matches perfectly with the reduced peak in the F 1*s* XAS, suggesting that the U 5*f*–F 2*p* hybridization has been reduced relative to the U 5*f*–O 2*p* hybridization in the uranium dioxide. Note that the major peaks in both the F 1*s* XAS and the U 4*d* XES have shifted together, retaining their overlap. This suggests that the U 6*d*–F 2*p* hybridization remains intact. (The U 6*d*-derived peak in the U 4*d* XES is caused by a two-electron process, as discussed in Refs. [1] and [7].) This hypothesis is confirmed by the placement of the U 2*p* XAS in the vicinity of the main F 1*s* XAS and U 4*d* XES peaks.

At this point it is useful to look at the internal structure of the U L_3 peak. This has been done in detail in Ref. [12] for both UO_2 and UF_4, so here only the pertinent aspects are summarized. Cluster calculations by Teterin *et al.* provide a histogrammatic UDOS for uranium tetrafluoride and uranium dioxide [25,26]. For UF_4, using Doniach-Sunjic line shapes [27] and assuming equal intensities, the smaller yellow curves are generated as shown in Fig. 3, along with the sum shown as the larger, broader curve. Clearly, some of these 6*d* states in the UDOS fall directly below the F 1*s* XAS main peak and above the U 4*d* XES main peak, thus confirming the assignment as U 6*d*–F 2*p* hybridization. The FEFF XANES calculations (not shown) confirm this assignment.

IV. CONCLUSION

By changing the oxidizing agent, it is possible to enhance (UO_2) or diminish (UF_4) the U 5*f*–2*p* hybridization. The highly electronegative F drives the system towards ionic behavior, while the dioxide exhibits strong U 5*f*–O 2*p* hybridization. The U 6*d*–2*p* hybridization persists, even in the ionic UF_4. Clearly, the UO_2 is a U 5*f*–O 2*p* covalent material. This result provides a powerful benchmarking for calculations of the electronic structure of uranium dioxide and enhances the likelihood of the accuracy of safety simulations based upon our understanding of the uranium dioxide electronic structure. Further, there is an important application to more highly radioactive samples here: the 4*d* XES is feasible with either photon or electron excitation, so in-house experiments upon highly radioactive Np, Pu, and Am samples are possible. The relative magnitude or the two U 4*d* XES features can provide a direct measure of 5*f*–2*p* hybridization versus 6*d*–2*p* hybridization, without the need to take highly radioactive samples to synchrotron radiation light sources.

ACKNOWLEDGMENTS

Lawrence Livermore National Laboratory (LLNL) is operated by Lawrence Livermore National Security, LLC, for the U.S. Department of Energy, National Nuclear Security Administration, under Contract DE-AC52-07NA27344. Work at Lawrence Berkeley National Laboratory (LBNL) (C.H.B., D.K.S.) was supported by the Director of the Office of Science, Office of Basic Energy Sciences (OBES), Division of Chemical Sciences, Geosciences, and Biosciences (CSGB), Heavy Element Chemistry (HEC) Program of the U.S. Department of Energy under Contract No. DE-AC02-05CH11231. The ALS is supported by the Director of the Office of Science, OBES of the U.S. Department of Energy at LBNL under Contract No. DE-AC02-05CH11231. The Stanford Synchrotron Radiation Lightsource is a national user facility operated by Stanford University on behalf of the DOE, Office of Basic Energy Sciences. The UF_4 sample was originally prepared at Oak Ridge National Laboratory and provided to LLNL by J. S. Morrell of Y12 [9]. J.G.T. wishes to thank (1) Glenn Fox and the PRT Program at LLNL for support during his sabbatical at LBNL; (2) D.K.S. for his hosting of the sabbatical at GTSC/LBNL; and (3) C.H.B. for the opportunity to learn new hard x-ray skills and collect data in the middle of the night again.

[1] S.-W. Yu and J. G. Tobin, J. Electron Spectrosc. Relat. Phenom. **187**, 15 (2013), and references therein.
[2] I. L. Pegg, Phys. Today **68**, 33 (2015).
[3] M. L. Wald, *The New York Times*, p. A20, October 17, 2014.
[4] I. D. Prodan, G. E. Scuseria, and R. L. Martin, Phys. Rev. B **76**, 033101 (2007).
[5] L. Petit, A. Svane, Z. Szotek, W. M. Temmerman, and G. M. Stocks, Phys. Rev. B **81**, 045108 (2010).
[6] S.-W. Yu, J. G. Tobin, J. C. Crowhurst, S. Sharma, J. K. Dewhurst, P. Olalde-Velasco, W. L. Yang, and W. J. Siekhaus, Phys. Rev. B **83**, 165102 (2011).
[7] J. G. Tobin and S.-W. Yu, Phys. Rev. Lett., **107**, 167406 (2011).
[8] V. Gouverneur and K. Seppelt, Chem. Rev. **115**, 563 (2015), Fluorine Chemistry Special Issue and references therein; Fluorine, http://en.wikipedia.org/wiki/Fluorine.
[9] J. Tobin, J. Electron Spectrosc. Relat. Phenom. **194**, 14 (2014).
[10] J. G. Tobin, C. H. Booth, W. Siekhaus, and D. K. Shuh, J. Vac. Sci. Technol. A **33**, 033001 (2015).
[11] G. Kalkowski, G. Kaindl, W. D. Brewer, and W. Krone, Phys. Rev. B **35**, 2667 (1987).
[12] J. G. Tobin, S.-W. Yu, C. H. Booth, T. Tyliszczak, D. K. Shuh, G. van der Laan, D. Sokaras, D. Nordlund, T.-C. Weng, and P. S. Bagus, Phys. Rev. B **92**, 035111 (2015).
[13] J. J. Jia, T. A. Callcott, J. Yurkas, A. W. Ellis, F. J. Himpsel, M. G. Samant, J. Stohr, D. L. Ederer, J. A. Carlisle, E. A. Hudson, L. J. Terminello, D. K. Shuh, and R. C. C. Perera, Rev. Sci. Instrum. **66**, 1394 (1995).
[14] C. H. Booth, Yu Jiang, D. L. Wang, J. N. Mitchell, P. H. Tobash, E. D. Bauer, M. A. Wall, P. G. Allen, D. Sokaras, D. Nordlund, T.-C. Weng, M. A. Torrez, and J. L. Sarrao, Proc. Natl. Acad. Sci. USA **109**, 10205 (2012).
[15] C. H. Booth, S. A. Medling, Y. Jiang, E. D. Bauer, P. H. Tobash, J. N. Mitchell, D. K. Veirs, M. A. Wall, P. G. Allen, J. J. Kas, D. Sokaras, D. Nordlund, and T.-C. Weng, J. Electron Spectrosc. Relat. Phenom. **194**, 57 (2014).
[16] D. Sokaras, T.-C. Weng, D. Nordlund, R. Alonso-Mori, P. Velikov, D. Wenger, A. Garachtchenko, M. George, V. Borzenets, B. Johnson, T. Rabedeau, and U. Bergmann, Rev. Sci. Instrum. **84**, 053102 (2013).
[17] J. J. Bucher, P. G. Allen, N. M. Edelstein, D. K. Shuh, N. W. Madden, C. Cork, P. Luke, D. Pehl, and D. Malone, Rev. Sci. Instrum. **67**, 3361 (1996).
[18] B. W. Veal, D. J. Lam, H. Diamond, and H. R. Hoekstra, Phys. Rev. B **15**, 2929 (1977).
[19] M. Magnuson, S. M. Butorin, L. Werme, J. Nordgren, K. E. Ivanov, J.-H. Guo, and D. K. Shuh, Appl. Surf. Sci. **252**, 5615 (2006).
[20] D. L. Clark (unpublished).
[21] J. D. Ward, M. Bowden, C. Tom Resch, S. Smith, B. K. McNamara, E. C. Buck, G. C. Eiden, and A. M. Duffin [Geostand. Geoanal. Res. (to be published)].
[22] J. J. Rehr, J. J. Kas, F. D. Vila, M. P. Prange, and K. Jorissen, Phys. Chem. Chem. Phys. **12**, 5503 (2010).
[23] B. K. Teo, *EXAFS Basic Principles and Data Analysis* (Springer Verlag, New York, 1986).
[24] A. M. Duffin (private communication).
[25] Yu. A. Teterin, K. I. Maslakov, M. V. Ryzhkov, O. P. Traparic, L. Vukcevic, A. Yu. Teterin, and A. D. Panov, Radiochemistry **47**, 215 (2005).
[26] A. Yu. Teterin, Yu. A. Teterin, K. I. Maslakov, A. D. Panov, M. V. Ryzhkov, and L. Vukcevic, Phys. Rev. B **74**, 045101 (2006).
[27] J. G. Tobin and F. O. Schumann, Surf. Sci. **478**, 211 (2001).